Preparation of Au/Pt Bimetallic Nanoparticles in Water-in-Oil Microemulsions

Ming-Li Wu, Dong-Hwang Chen,* and Ting-Chia Huang

Department of Chemical Engineering, National Cheng Kung University, Tainan, Taiwan 701, Republic of China

Received August 14, 2000. Revised Manuscript Received November 28, 2000

The preparation and characterization of bimetallic nanoparticles at various molar ratios of Au/Pt by the coreduction of chloroauric and chloroplatinic acid with hydrazine in the water-in-oil microemulsions of water/AOT/isooctane at 25 °C were described. The Au/Pt bimetallic nanoparticles prepared using feeding solutions with the concentration ratios of $[HAuCl_4]/[H_2PtCl_6] = {}^9/_1-{}^1/_9$ essentially were monodispersed and had mean diameters of 3−4.5 nm. Both the UV/vis absorption spectra and XRD patterns of the bimetallic systems and the physical mixtures of individual metallic nanoparticles suggested the formation of bimetallic nanoparticles. The EDX analysis on individual particles confirmed the presence of two metals in a particle. It was indicated that the composition for each particle was roughly consistent with that of the feeding solution. The XPS analysis showed that the resultant Au/Pt bimetallic nanoparticles had a structure of Au-core/Pt-shell and their surface composition varied linearly with that of the feeding solution. The investigations on the size and formation kinetics of particles suggested that the reduction of $AuCl_4^-$ and $PtCl_6^{-2}$ ions was almost finished before the formation of nuclei, the size of the bimetallic nanoparticles was determined by number of the nuclei formed at the very beginning of reaction, and the nucleation rate of Au was much faster than that of Pt. Furthermore, the nuclei for the bimetallic system might be composed of Au and Pt. Accordingly, a formation process for the Au/Pt bimetallic nanoparticles was suggested.

Introduction

Recently, intense research has been focused on nanoparticles because they exhibit unusual chemical and physical properties different from those of relatively larger particles[1−3] and have many potential applications in the fields of optoelectronics, semiconductors, catalysts, photocatalysts, magnetic materials, drug delivery, and so on.[4−6] Bimetallic nanoparticles have been particularly attractive due to the improvement of catalytic properties[7] and the change of surface plasma band energy[8] relative to the separate metals. It is of great interest and a challenge to prepare bimetallic nanoparticles with a controlled composition distribution.

Several methods have been used to prepare bimetallic nanoparticles, including alcohol reduction,[7,9] citrate reduction,[8c,10] the polyol process,[11] solvent extraction reduction,[8b,12] the sonochemical method,[13] photoreduction,[14] decomposition of organometallic precursors,[15] and electrolysis of bulk metals.[16] Control of particle size has been achieved by the presence of protective agents such

* Telephone: 886-6-2757575 ext. 62680. Fax: 886-6-2344496. E-mail: chendh@mail.ncku.edu.tw.

(1) (a) Ozin, G A. *Adv. Mater.* **1992**, *4*, 612. (b) Cahn, R. W. *Nature* **1992**, *359*, 591. (c) Ozin, G. A. *Science* **1996**, *271*, 920.

(2) (a) Hayashi, C. *Phys. Today* **1987**, *40*, 44. (b) Gleiter, H. *Prog. Mater. Sci.* **1989**, *33*, 223.

(3) (a) Fendler, J. H. *Chem. Rev.* **1987**, *87*, 877. (b) Henglein, A. *Chem. Rev.* **1989**, *89*, 1861. (c) Schimid, G. *Clusters and Colloids: From Theory to Application*; VCH: Weinheim, 1994.

(4) (a) Toshima, N.; Yonezawa, T. *New J. Chem.* **1998**, 1179. (b) Beecroft, L. L.; Ober, C. K. *Chem. Mater.* **1997**, *9*, 1302. (c) Han, Y. T. *MRS Bull.* **1989**, *14*, 13. (d) Siegel, R. W. *MRS Bull.* **1990**, *15*, 60.

(5) (a) Schmid, G. *Chem. Rev.* **1992**, *92*, 1709. (b) Kamat, P. V. *Chem. Rev.* **1993**, *93*, 267. (c) Lewis, L. N. *Chem. Rev.* **1993**, *93*, 2693. (d) Gates, B. C. *Chem. Rev.* **1995**, *95*, 511.

(6) (a) Brus, L. *J. Phys. Chem.* **1986**, *90*, 2555. (b) Hoffman, A. J.; Mils, G.; Yee, H.; Hoffman, M. R. *J. Phys. Chem.* **1995**, *99*, 4414. (c) Lee, A. F.; Baddeley, C. J.; Hardacre, C.; Ormerod, R, M.; Lambert, R. M.; Schmid, G.; West, H. *J. Phys. Chem.* **1995**, *99*, 6096.

(7) (a) Toshima, N.; Yonezawa, T.; Kushihashi, K. *J. Chem. Soc., Faraday Trans.* **1993**, *89*, 2537. (b) Toshima, N.; Harada, M.; Yamazaki, Y.; Asakura, K. *J. Phys. Chem.* **1992** *96*, 9927. (c) Harada, M.; Asakura, K.; Ueki, Y.; Toshima, N. *J. Phys. Chem.* **1993**, *97*, 5103. (d) Wang, Y.; Toshima, N. *J. Phys. Chem. B* **1997**, *101*, 5301.

(8) (a) Belloni, J.; Mostafavi, M.; Remita, H., Marignier, J. L.; Delcourt, M. O. *New J. Chem.* **1998**, 1293. (b) Han, S. W.; Kim, Y.; Kim, K. *J. Colloid Interface Sci.* **1998**, *208*, 272. (c) Link, S.; Wang, Z. L.; El-Sayed, M. A. *J. Phys. Chem. B* **1999**, *103*, 3529.

(9) (a) Yonezawa, T., Toshima, N. *J. Chem. Soc., Faraday Trans.* **1995**, *91*, 4111. (b) Yonezawa, T.; Toshima, N. *J. Mol. Catal.* **1993**, *83*, 167. (c) Toshima, N.; Harada, M.; Yonezawa, T.; Kushihashi, K.; Asakura, K. *J. Phys. Chem.* **1991**, *95*, 7448. (d) Toshima, N.; Kushihashi, K.; Yonezawa, T.; Hirai, H. *Chem. Lett.* **1989**, 1769. (e) Toshima, N.; Wang, Y. *Langmuir* **1994**, *10*, 4574. (f) Harada, M.; Asakura, K.; Ueki, Y.; Toshima, N. *J. Phys. Chem.* **1993**, *97*, 10742.

(10) Miner, R. S.; Namba, S.; Turkevich, J. In *Proceedings of the 7th International Congress on Catalysis*; Kodansha: Tokyo, 1981.

(11) Silvert, P.-Y.; Vijayakrishnan, V.; Vibert, P.; Herrera-Urbina, R.; Elhsissen, K. T. *Nanostruct. Mater.* **1996**, *7*, 611.

(12) Esumi, K.; Shiratori, M.; Ishizuka, H.; Tano, T.; Torigoe, K.; Meguro, K. *Langmuir* **1991**, *7*, 457.

(13) Mizukoshi, Y.; Okitsu, K.; Maeda, Y.; Yamamoto, T. A.; Oshima, R.; Nagata, Y. *J. Phys. Chem. B* **1997**, *101*, 7033.

(14) Remita, S.; Mostafavi, M.; Delcourt, M. O. *Radiat. Phys. Chem.* **1996**, *47*, 275.

(15) (a) Bradley, J. S.; Hill, E. W.; Klein, C.; Chaudret, B.; Duteil, A. *J. Chem. Mater.* **1993**, *5*, 254. (b) Pan, C.; Dassenoy, F.; Casanove, M. J.; Philippot, K.; Amiens, C.; Lecante, P.; Mosset, A.; Chaudret, B. *J. Phys. Chem. B* **1999**, *103*, 10098.

(16) (a) Reetz, M. T.; Helbig, W.; Quaiser, S. A. *J. Chem. Mater.* **1995**, *7*, 2227. (b) Reetz, M. T.; Quaiser, S. A. *Angew. Chem., Int. Ed. Engl.* **1995**, *34*, 2240.

10.1021/cm0006502 CCC: $20.00
Published on Web 01/13/2001

as soluble polymers and organic ligands, or by the adsorption of anions on the particle surface. It has been shown that the size, structure, and composition distribution of the resultant particles depended on the preparation conditions.

Water-in-oil (w/o) microemulsions are transparent, isotropic, thermodynamically stable liquid media with nanosized water droplets dispersed in a continuous oil phase and stabilized by surfactant molecules at the water/oil interface. The surfactant-stabilized water pools provide a microenvironment for the preparation of a nanoparticle by exchanging their contents via the fusion−redispersion process and preventing the excess aggregation of particles. As a result, the particles obtained in such a medium are generally very fine and monodispersed. Many kinds of nanoparticles have been prepared in w/o microemulsions, including metals,[17−22] metal oxides and hydroxides,[23−27] metal sulfides and selenides,[28−32] metal borides,[33] metal carbonates,[34] and organic polymers.[35] However, the preparation of bimetallic nanoparticles in w/o microemulsions has not been tried as much except for the Pt/Pd[36] and Cu/Au[37] systems.

Au/Pt bimetallic nanoparticles have received significant attention because of their special catalytic properties. Some articles have described their preparation by citrate reduction,[10,38] photoreduction,[14] and alcohol reduction.[9b] Their preparation by microemulsion processing has not been reported. In this paper, the preparation of Au/Pt bimetallic nanoparticles in w/o microemulsions of water/AOT/isooctane by the coreduction of chloroauric and chloroplatinic acid with hydrazine at 25 °C is reported. The size, structure, optical properties, and composition distribution of the resultant nanoparticles were characterized by transmission electron microscopy (TEM), X-ray diffraction (XRD), UV/vis spectroscopy, energy-dispersive X-ray analysis (EDX), and X-ray photoelectron spectroscopy (XPS). The effects of the preparation conditions including the concentrations of precursors and the molar ratio of water to surfactant were investigated. Also, the formation process for bimetallic nanoparticles was discussed.

Experimental Section

Materials. Hydrogen tetrachloraurate(III) hydrate, hydrochloric acid solution, and hydrazinium hydroxide were guaranteed reagents of E. Merck (Darmstadt). Hydrogen hexachloroplatinate(IV) hydrate was obtained from Across Organics (Belgium). Sodium di-2-ethylhexylsulfosuccinate (AOT), purchased from Sigma Chemical Co. (St. Louis, MO), was vacuum-dried at 60 °C for 24 h and stored in a vacuum desiccator before use. HPLC-grade isooctane, supplied by TEDIA (Fairfield), was dehydrated with 4 Å molecular sieves (8−12 mesh, Jansseu) for at least 24 h and kept in a vacuum desiccator prior to use. The residual water of the AOT/isooctane solution was recognized to be negligible by using a Karl-Fisher moisture titrator (Kyoto Electronics MKC-50). The water used throughout this work was reagent-grade water produced by a Milli-Q SP ultrapure-water purification system of Nihon Millipore Ltd., Tokyo.

The w/o microemulsion solutions containing hydrazine or a mixture of $HAuCl_4/H_2PtCl_6$ at a specified molar ratio were prepared by injecting the required amount of the corresponding aqueous solutions into an isooctane solution of AOT, and were then used for the preparation of nanoparticles within a few minutes.

Preparation of Metallic Nanoparticles. The preparation of bimetallic and individual metallic nanoparticles was achieved by mixing equal volumes of two w/o microemulsion solutions at the same molar ratio of water to AOT (ω_0) and AOT concentration, one containing an aqueous solution of the metal salts and the other containing an aqueous solution of hydrazine. The reduction of $HAuCl_4$ and H_2PtCl_6 was as follows:

$$4HAuCl_4 + 3N_2H_5OH \rightarrow 4Au + 16HCl + 3N_2 + 3H_2O \quad (1)$$

$$H_2PtCl_6 + N_2H_5OH \rightarrow Pt + 6HCl + N_2 + H_2O \quad (2)$$

A preliminary study indicated that the nanoparticles usually reached their final sizes within 1 h. Thus, the samples for various analyses were taken after about 3 h. In this work the concentration of AOT was based on the overall volume of the reverse micellar solution, while the concentrations of the metal salts and hydrazine were referred to the volume of aqueous solution added in the w/o microemulsion solution. In this study, the concentrations of AOT, hydrazine, and the total metal salts were fixed at 0.1, 1.0, and 0.1 M, respectively. The temperature was kept at 25 °C, and unless otherwise specified, the ω_0 value was 6.0.

Characterization. The particle sizes were determined by transmission electron microscopy (TEM) using a JEOL model JEM-1200EX at 80 kV. The sample for TEM analysis was obtained by placing a drop of the colloidal solution onto a Formvar-covered copper grid and evaporating it in air at room temperature. Before the samples were withdrawn, the colloidal solutions were sonicated for 1 min to obtain a better particle dispersion on the copper grid. For each sample, usually over 100 particles from different parts of the grid were used to estimate the mean diameter and size distribution of particles. The samples were also used to determine the elemental ratios of particles by energy-dispersive X-ray (EDX) analysis with the system attached to a Hitachi model HF-2000 field emission transmission electron microscope. X-ray diffraction (XRD) measurements were performed on a Rigaku D/max V X-ray diffractometer using Cu Kα radiation (λ = 0.1542 nm). The

(17) Boutonnet, M.; Kizling, J.; Stenius, P.; Maire, G. *Colloids Surf.* **1982**, *5*, 209.
(18) Petit, C.; Lixon, P.; Pilei, M.-P. *J. Phys. Chem.* **1993**, *97*, 12974.
(19) Robinson, B. H.; Khan-Iodhi, A. N.; Towey, T. In *Structure and Reactivity in Reverse Micelles*; Pileni, M. P., Ed.; Elsevier: Amsterdam, 1989.
(20) Qi, L.; Ma, J.; Shen, J. *J. Colloid Interface Sci.* **1997**, *186*, 498.
(21) (a) Chen, D. H.; Wang, C. C.; Hung, T. C. *J. Colloid Interface Sci.* **1999**, *210*, 123. (b) Chen, D. H.; Yeh, J. J.; Hung, T. C. *J. Colloid Interface Sci.* **1999**, *215*, 159.
(22) Chen, D. H.; Wu, S. H. *Chem. Mater.* **2000**, *12*, 1354.
(23) Osseo-Asare, K.; Arriagada, F. *J. Colloid Interface Sci.* **1990**, *50*, 321.
(24) Pillai, V.; Kumar, P.; Multani, M. S.; Shah, D. O. *Colloid Surf. A* **1993**, *80*, 69.
(25) Joselevich, E.; Willner, I. *J. Phys. Chem.* **1994**, *98*, 7628.
(26) Chhabra, V.; Lal, M.; Maitra, A. N.; Ayyub, P. *Colloid Polym. Sci.* **1995**, *273*, 939.
(27) Chang, C. L.; Fogler, H. S. *Langmuir* **1997**, *13*, 3295.
(28) Lianos, P.; Thomas, J. K. *J. Colloid Interface Sci.* **1987**, *117*, 505.
(29) Kortan, A. R.; Hull, R.; Opila, R. L.; Bawendi, M. G.; Steigerwald, M. L.; Carroll, P. J.; Brus, L. E. *J. Am. Chem. Soc.* **1990**, *112*, 1327.
(30) Ward, A. J.; O'Sullivan, E. C.; Rang, J.-C.; Nedeljkovic, J.; Patel, R. C. *J. Colloid Interface Sci.* **1993**, *161*, 316.
(31) Hirai, T.; Shiojiri, S.; Komasawa, I. *J. Am. Chem. Eng. Jpn.* **1994**, *27*, 590.
(32) Haram, S. K.; Mahadeshwar, A. R.; Dixit, S. G. *J. Phys. Chem.* **1996**, *100*, 5868.
(33) Nagy, J. *J. Colloids Surf.* **1989**, *35*, 201.
(34) Kandori, K.; Kon-No, K.; Kitahara, A. *J. Colloid Interface Sci.* **1988**, *122*, 78.
(35) Antonietti, M.; Basten, R.; Lonmann, S. *Macromol. Chem. Phys.* **1995**, *196*, 441.
(36) Touroude, R.; Girard, P.; Maire, G.; Kizling, J.; Boutonnet-Kizling, M.; Stenius, P. *Colloids Surf.* **1992**, *67*, 9.
(37) Sangregorio, C.; Galeotti, M.; Bardi, U.; Baglioni, P. *Langmuir* **1996**, *12*, 5800.
(38) Schimid, G.; Lehnert, A.; Malm, J. O.; Bovin, J O. *Angew. Chem., Int. Ed. Engl.* **1991**, *30*, 874.

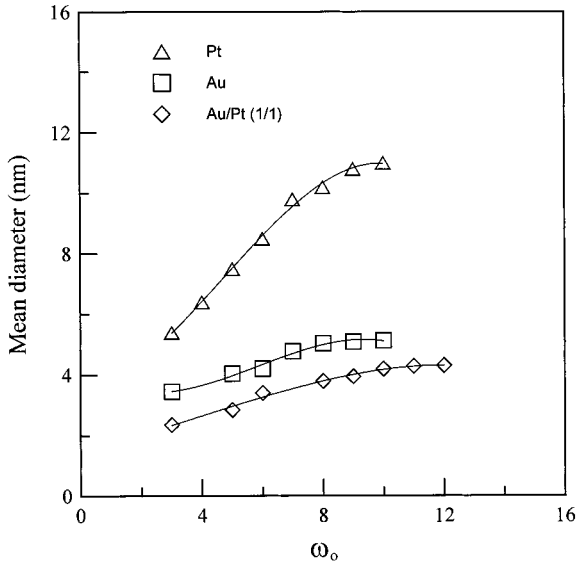

Figure 1. Effect of ω_0 value on the size of Au, Pt, and Au/Pt bimetallic nanoparticles synthesized in water/AOT/isooctane reverse micelles. Reaction conditions: [metal salts] = 0.1 M; [N_2H_5OH] = 1.0 M; [AOT] = 0.1 M; reaction time = 3 h.

samples for XRD analysis were prepared by first adding thiophenol to the w/o microemulsion solutions (i.e., [thiophenol]/[metal] = $^2/_1$) to cause phase separation, then centrifuging the mixtures, washing the precipitates with isooctane and ethanol, and finally drying the obtained precipitates at room temperature. After dispersing the precipitates in isooctane and depositing the thiophenol-capped particles on a graphite support by solvent evaporation at room temperature, the obtained samples were further used for the XPS measurements by a Fison (VG) ESCA 210 spectrometer equipped with a Mg Kα X-ray source. The UV/vis spectra of the w/o microemulsion solutions containing various nanoparticles were measured after 3 h by a Hitachi U-3000 spectrophotometer equipped with a 10 mm quartz cell. During the formation of the Au nanoparticles, the absorbance change of the w/o microemulsion solution with reaction time at 520 nm was measured in a stopped-flow spectrophotometer (Union Giken, RA401).

Results and Discussion

Particle Sizes. As is known, when the particle diameter reaches that of the microemulsion droplet, surfactant molecules can adsorb on the surface of the particle formed therein and restrict the growth of the nanoparticles. Therefore the effect of the ω_0 value, a size-determining key parameter of microemulsion droplets, on the particle size was first investigated. As shown in Figure 1, the sizes of the Au, Pt, and Au/Pt ($^1/_1$) bimetallic nanoparticles exhibited similar tendencies: increasing with an increase in the ω_0 value. This result could be reasonably explained by the increase in the size of the microemulsion droplets. The conditions for $\omega_0 >$ 12 were not investigated because the aqueous solution of metal salts could not be solubilized completely into the AOT/isooctane solution. In addition, it was noticed that the Au/Pt ($^1/_1$) bimetallic nanoparticles were significantly smaller than both the Au and Pt nanoparticles over the whole ω_0 range examined. This might relate to the nucleation process of the particles and is discussed further later.

The TEM micrographs and the size distributions of nanoparticles obtained at various molar ratios of Au/Pt are shown in Figure 2. Not only Au and Pt but also Au/Pt bimetallic particles were very fine and essentially monodispersed. Since the difference in the mean diameter of the Au (4.2 nm) and Pt (8.3 nm) particles was large enough to distinguish, the monodispersion of the bimetallic system suggested that they are not physical mixtures of the individual metallic nanoparticles and that bimetallic nanoparticles were really formed.

The mean diameters of Au, Pt, and the bimetallic nanoparticles at various molar ratios of Au and Pt are illustrated in Figure 3. It was found that the mean diameters of the bimetallic nanoparticles varied with the molar ratios of Au/Pt and showed a minimum at a Pt mole fraction of 25%. The influence of composition on particle size also has been reported. Yonezawa and Toshima found that the mean diameters of the bimetallic nanoparticles depended on the compositions and showed a negative deviation for the Pd/Pt, Au/Pd, and Au/Pt systems prepared by alcohol reduction,[9a] whereas a positive deviation was observed by Esumi et al. for the Pd/Pt system prepared by solvent extraction reduction.[12] Although these results were not completely consistent, they all were referred to a difference in the nucleation process, which could be affected by the kinds of materials, the reaction media, and the preparation conditions.

As is well-known, in addition to the collision energy and the sticking coefficient, the rates of nucleation and growth are determined mainly by the probabilities of the collisions between several atoms, between one atom and a nucleus, and between two or more nuclei. The former kind of collision is related to the nucleation and the latter two kinds of collision to the growth process. When the reduction rate was so large that almost all of the ions were reduced before the formation of nuclei and the probability of the effective collision between one atom and a nucleus were much higher than those of the other two collisions, the size of the resultant particles would be monodispersive and determined by the number of the nuclei formed at the very beginning of the reaction. Thus, in this work, the reduction of the $AuCl_4^-$ and $PtCl_6^{-2}$ ions might be so fast that they are reduced almost completely before the formation of nuclei. Furthermore, the sizes of the Au, Pt, and Au/Pt bimetallic nanoparticles obtained are determined by their nucleation processes. Since the total concentration of metal ions was fixed, the smaller sizes of the Au/Pt bimetallic nanoparticles relative to the individual Au and Pt nanoparticles revealed that more nuclei were formed at the very beginning of the reaction. This seems to imply that the number of atoms (Au and Pt) required to form a nucleus was dependent on the composition and was lower except at high Pt contents. Therefore, it is suggested that the nuclei for the formation of Au/Pt bimetallic nanoparticles in this work might be composed of both Au and Pt atoms. This is based on the reasoning that the total Gibbs energy of an atomic assembly might vary with the composition due to the different bond enthalpies or interactions of Au−Au, Pt−Pt, and Au−Pt and hence lead to the number of atoms required for the formation of a nucleus being different at different compositions. Another possible condition is that the nuclei were composed of only Au atoms but the number of Au atoms required to form a stable nucleus was reduced due to the presence of the Pt atoms in the

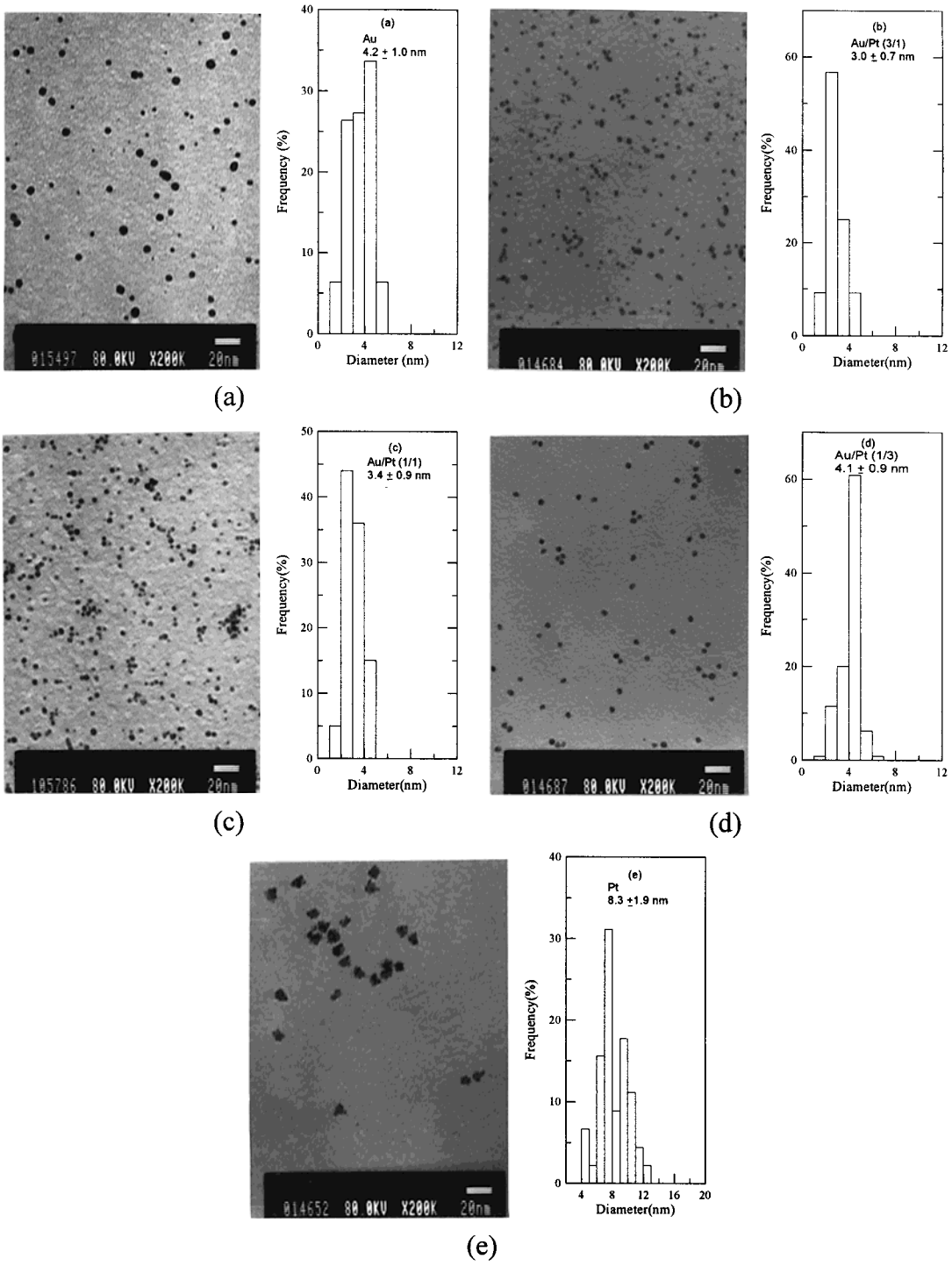

Figure 2. Transmission electron micrographs and particle size distributions of the individual metallic and bimetallic nanoparticles: (a) Au, (b) Au/Pt ($^3/_1$), (c) Au/Pt ($^1/_1$), (d) Au/Pt ($^3/_1$), and (e) Pt. Reaction conditions as in Figure 1 and with $\omega_0 = 6$.

solution. However, based on the probability of the atomic assembly and the reasoning that the Pt atoms should have stronger influence on the total Gibbs energy of an atomic assembly when they were present in a nucleus than when they were just present in the solution, the former suggestion that the nuclei might be composed of both Au and Pt atoms is favored.

UV/vis Absorption Spectra. Figure 4 shows the UV/vis absorption spectra of the bimetallic nanoparticles and the physical mixtures of Au and Pt monometallic nanoparticles. The absorption spectra for the physical mixtures show an absorption peak at about 520 nm. This absorption peak is a surface plasma absorption due to Au, and its area decreases with a decrease in the Au/Pt ratio. For the bimetallic systems, no significant surface plasma absorption was observed, even at a Au/Pt molar ratio of $^9/_1$. This reveals that the bimetallic systems are not physical mixtures of the individual metals. Furthermore, the sudden disappearance of the surface plasma absorption of Au implies that the surface of the Au/Pt bimetallic nanoparticles obtained in this work has more Pt atoms than the inner core. A similar phenomenon was also observed by Yonezawa and Toshima,[9b] although the disappearance of the surface

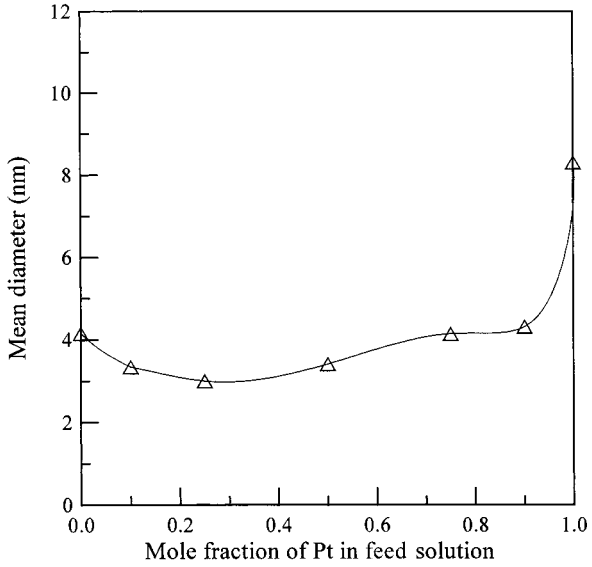

Figure 3. Mean diameters of Au/Pt bimetallic nanoparticles as a function of composition in feeding solution. Reaction conditions as in Figure 2.

plasma absorption of Au was not so sudden in their work due to the different preparation method employed.

Structure. As described in the Experimental Section, thiophenol-capped nanoparticles were prepared for XRD analysis. It was found that the particles could be well dispersed in a mixture of pyridine and 1,2-dichloroethane, and their sizes were essentially the same as those of uncapped ones on the basis of the TEM analysis. Thus, it can be ensured that the structure of particles is not changed due to the sample preparation.

Figure 5a shows the XRD patterns of the Au, Pt, the physical mixture of Au and Pt ($^1/_1$), and the Au/Pt ($^1/_1$) bimetallic nanoparticles. The characteristic peaks for Au ($2\theta = 38.2$ and 44.4) and those for Pt ($2\theta = 39.8$ and 46.2), marked by their indices ((111) and (200)), were observed. This revealed that the resultant Au and Pt particles were in the face-centered cubic (fcc) structure, although the broad peaks showed they were poorly crystalline, resulting from less ordered structures as is usually observed for nanoparticles. For the physical mixture of Au and Pt nanoparticles, both the characteristic peaks of Au and Pt were observed without a shift. However, only one broad peak between those of Au ($2\theta = 38.2$) and Pt ($2\theta = 39.8$) was observed for the Au/Pt ($^1/_1$) bimetallic system. This also suggests the formation of bimetallic nanoparticles. In addition, in Figure 5b, a continuous drift of the peak from that of Au to that of Pt is observed. This feature implies that the composition of each bimetallic particle is proportional to that of the feed solution.

Compositional Analysis. For each molar ratio of Au/Pt, four particles on the copper grid were chosen randomly to analyze the composition in each particle by EDX. The result is indicated in Table 1. The deviation of composition among different particles at each composition of feed solution might be caused by detection errors because the particles were too fine. In addition, the average compositions are observed to be roughly in agreement with those of the two metal salts in their aqueous solutions. The deviation could be due to the low number of particles chosen for analysis and

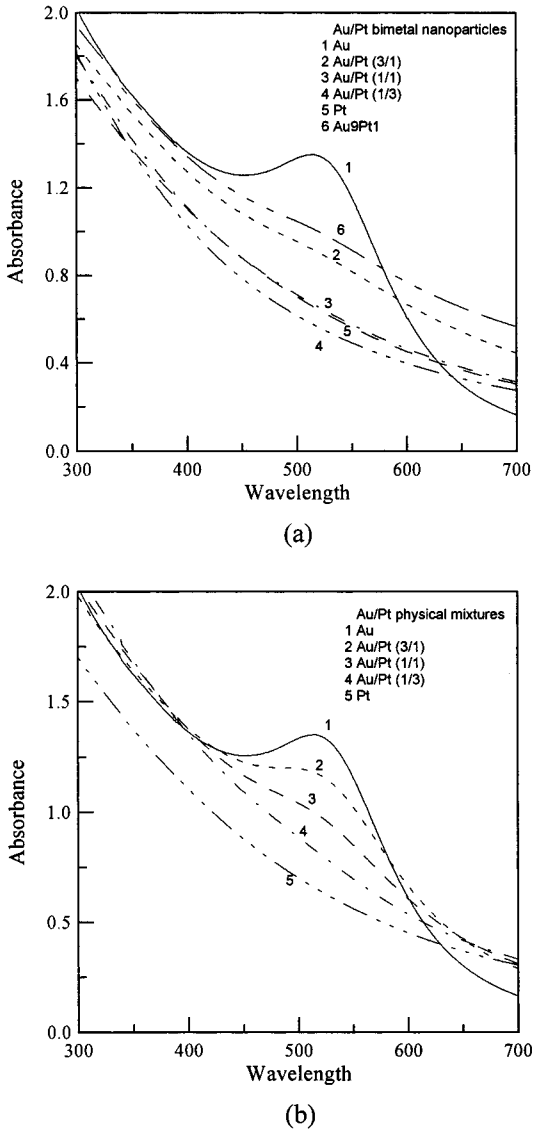

Figure 4. UV/vis absorption spectra of Au/Pt bimetallic nanoparticles (a) and the physical mixtures of individual Au and Pt nanoparticles (b) at various molar ratios. Reaction conditions as in Figure 2.

to detection errors. In any case, the EDX analysis confirms directly the formation of Au/Pt bimetallic nanoparticles.

To further investigate the composition distribution in a particle, the surface compositions of bimetallic nanoparticles were measured. Figure 6 shows a typical XPS spectra of the Au_{4f} and Pt_{4f} regions of the thiophenol-capped Au/Pt ($^1/_3$) bimetallic nanoparticles. Similar results were obtained for other bimetallic particles at various molar ratios of Au/Pt. The XPS data are summarized in Table 2. On the basis of the intensities of the XPS peaks, the elemental ratios of Au/Pt on the surfaces of the bimetallic nanoparticles could be obtained. The results are indicated in Table 2 and plotted in Figure 7. It was found that the Pt atoms were enriched on the surface of the Au/Pt bimetallic nanoparticles. This is consistent with the observations of the UV/vis absorption spectra. Furthermore, the surface composition of bimetallic nanoparticles varies linearly with the composition in the feeding solution within the composition range examined. This suggests that the

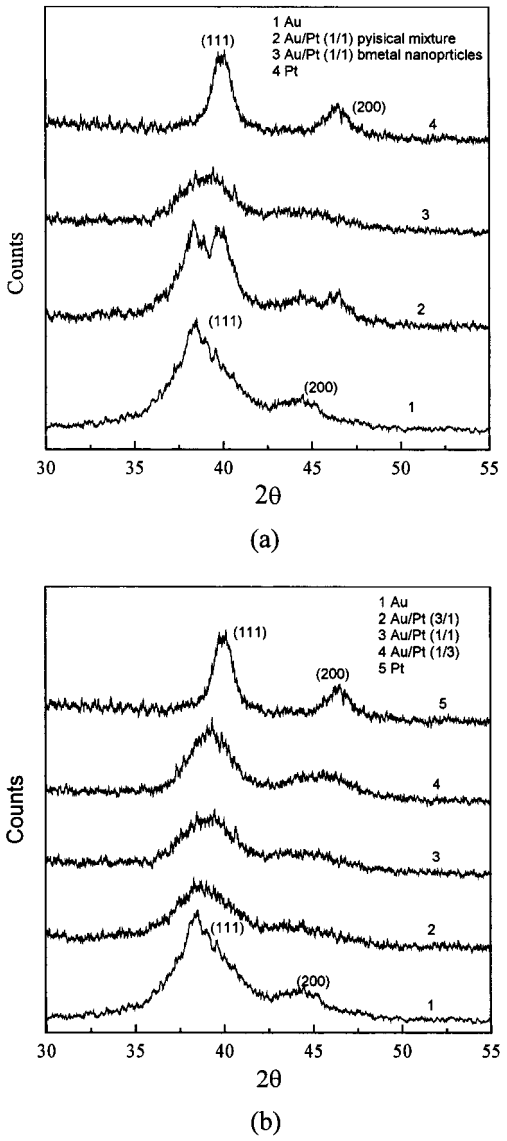

Figure 5. XRD patterns of the physical mixtures of individual Au and Pt nanoparticles and the Au/Pt bimetallic nanoparticles at various molar ratios. Reaction conditions as in Figure 2.

Table 1. Elemental Ratio in an Au/Pt Bimetallic Nanoparticle Chosen Randomly on the Copper Grid Measured by EDX

feeding soln[a]	elemental ratio (Au/Pt) in a particle				
	1	2	3	4	ave.
$^3/_1$	72.1/27.9	78.1/21.9	75.0/25.0	78.9/21.1	76.0/24.0
$^1/_1$	65.2/34.8	52.5/47.5	69.0/31.0	46.3/53.7	58.2/42.8
$^1/_3$	31.6/68.4	30.5/69.5	31.1/68.9	33.8/66.2	31.7/69.3

[a] [HAuCl4]/[H2PtCl6].

resultant bimetallic nanoparticles had a structure of Au-core/Pt-shell. This could be attributed to the formation process that is described further in the following section. In addition, it should be mentioned that the surface composition of the bimetallic nanoparticles can be controlled by the feeding composition. This should be of the interest for the preparation of catalysts.

Formation Process of the Particles. By observing the formation process of the particles, it was found that the color of the reaction solution turned from yellow to red instantaneously for the preparation of the Au nanoparticles. As shown in Figure 8, the Au nanoparticles reached their final sizes so quickly that the required time could not be detected by conventional methods. A stopped-flow spectrophotometer was hence used to measure the formation rate of the Au nanoparticles. As shown in Figure 9, the absorbance at 520 nm,

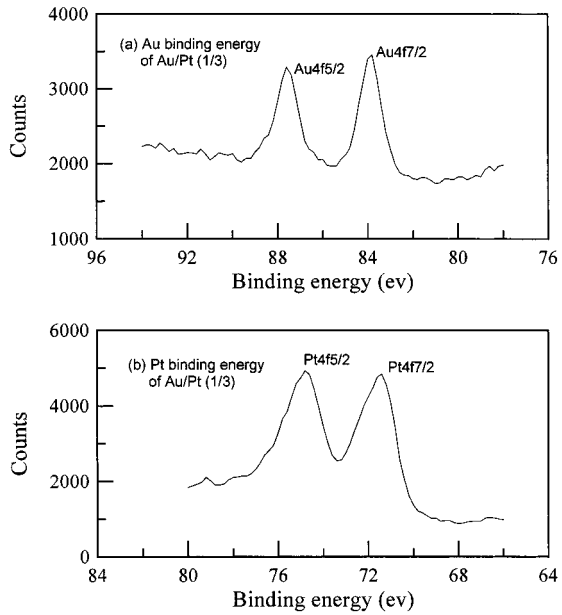

Figure 6. XPS spectra of Au 4f (a) and Pt 4f (b) regions for the thiophenol-capped Au/Pt ($^1/_3$) bimetallic nanoparticles. Reaction conditions as in Figure 2 and with [thiophenol]/[metals] = $^2/_1$.

Table 2. Quantitative XPS Data of Thiophenol-Capped Au/Pt Bimetallic Nanoparticles

feeding soln[a]	binding energy (ev)[b]	elem. ratio (Au/Pt) on particle surface
$^4/_0$	$Au_{4f7/2}$ = 84.2	
$^9/_1$	$Au_{4f7/2}$ = 84.3, $Pt_{4f7/2}$ = 71.6	6.69/1
$^3/_1$	$Au_{4f7/2}$ = 84.2, $Pt_{4f7/2}$ = 71.6	2.70/1
$^1/_1$	$Au_{4f7/2}$ = 84.1, $Pt_{4f7/2}$ = 71.4	1/1.18
$^1/_3$	$Au_{4f7/2}$ = 84.1, $Pt_{4f7/2}$ = 71.4	1/4.95
$^1/_9$	$Au_{4f7/2}$ = 84.2, $Pt_{4f7/2}$ = 71.6	1/17.18
$^0/_4$	$Pt_{4f7/2}$ = 71.7	

[a] [HAuCl4]/[H2PtCl6]. [b] The values of binding energy are determined with respect to the C_{1s} peak.

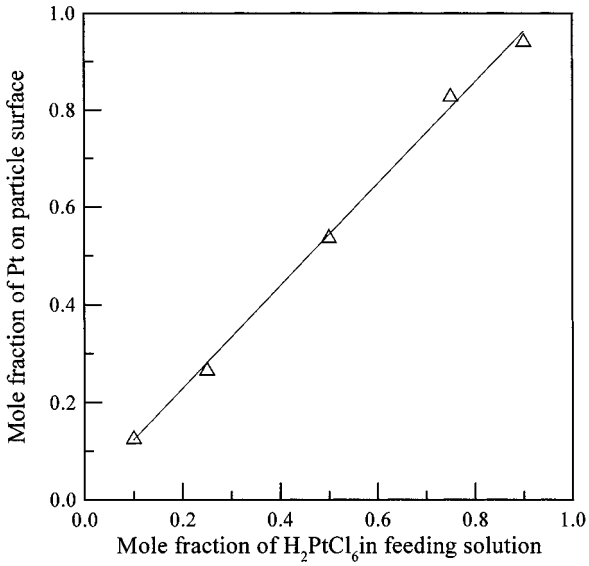

Figure 7. Relationship between Pt content on the particle surface and that in feeding solution.

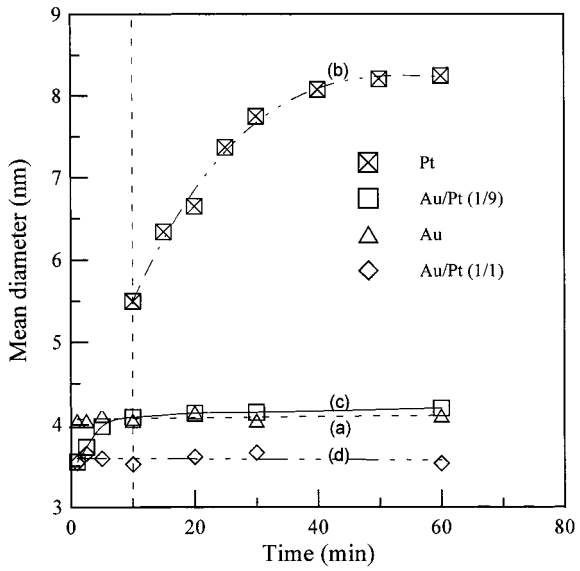

Figure 8. Variation of mean diameter with reaction time. (a) Au, (b) Pt, (c) Au/Pt ($^1/_9$), and (d) Au/Pt ($^1/_1$). Reaction conditions as in Figure 2.

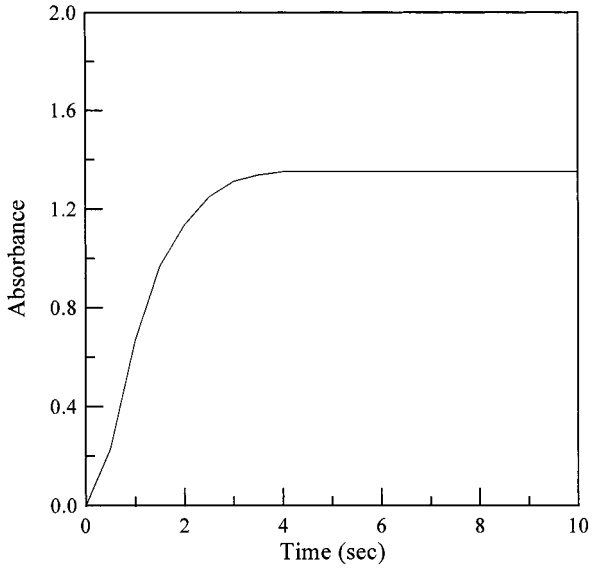

Figure 9. Absorbance change with reaction time at a wavelength of 520 nm measured by a stopped-flow spectrophotometer. Reaction conditions: $[HAuCl_4] = 0.1$ M; $[N_2H_5OH] = 1.0$M; $\omega_0 = 6$; [AOT] = 0.1M.

which is the characteristic peak of Au, increased first and then approached a constant value after about 4 s. This reveals that the formation of Au nanoparticles is completed in 4 s. In the case of the Pt nanoparticles, the color of the reaction solution turned from light yellow to colorless instantaneously and remained unchanged for about 7 min. In this period, no particles were observed by TEM analysis. In the following 7−60 min, the color of solution gradually turned to brown and reached a stable condition. As indicated in Figure 8, the Pt nanoparticles grew gradually to their final size in this period. Thus, the instantaneous disappearance of light yellow suggests that the reduction of H_2PtCl_6 was quite fast, and the colorless and the following periods could be associated with the nucleation and growth of the particles, respectively. This was consistent with the suggestion mentioned in the investigation of the particle size: the reduction of $PtCl_6^{-2}$ ions was almost finished before the formation of nuclei. For both the cases of Au/Pt ($^1/_1$) and Au/Pt ($^1/_9$) bimetallic nanoparticles, the colors of the reaction solutions also turned from yellow to red instantaneously. However, as indicated in Figure 8, the Au/Pt ($^1/_1$) nanoparticles reach their final size very quickly, but the Au/Pt ($^1/_9$) nanoparticles reach their final size after about 10 min. This indicates that the nucleation and growth of Pt in the bimetallic system is accelerated, although they were still slower than those of Au. This could be attributed to the earlier formation of nuclei due to the presence of Au.

As mentioned above, the investigation of the particle size suggests that the reduction of the $AuCl_4^-$ and $PtCl_6^{-2}$ ions is almost finished before the formation of nuclei, and the nuclei for the formation of the Au/Pt bimetallic nanoparticles in this work might be composed of Au and Pt atoms. In addition, although it was not known whether the reduction of $AuCl_4^-$ ions was faster than that of $PtCl_6^{-2}$ ions, their reduction potentials shown below reveals that the $AuCl_4^-$ ions had the priority in reduction.

$$AuCl_4^- + 3e \rightarrow Au + 4Cl^- \quad 1.00\ V \qquad (3)$$

$$PtCl_6^{-2} + 2e \rightarrow PtCl_4^{-2} + 2Cl^- \quad 0.68\ V \qquad (4)$$

$$PtCl_4^{-2} + 2e \rightarrow Pt + 4Cl^- \quad 0.73\ V \qquad (5)$$

Thus, according to the above analyses and discussions, the formation process of the Au/Pt bimetallic nanoparticles can be described as follows. First, the $AuCl_4^-$ and $PtCl_6^{-2}$ ions are reduced completely. Then, the Au and Pd atoms start to aggregate to form the nuclei. Since the nucleation rate of Au is much faster than that of Pt, the nuclei of the bimetallic system should be formed initially by the conformation of Au atoms, and the composition of the nuclei might have a higher Au content than that of the feed solution. All nuclei might be formed almost at the same time. After this, the bimetallic nanoparticles grow gradually to their final size by the co-deposition of Au and Pt atoms on the nuclei, but since Au atoms should have the priority to deposit on the nuclei, this leads to the formation of a Au-core/Pt-shell structure.

Summary

Au/Pt bimetallic nanoparticles were prepared in microemulsions of water/AOT/isooctane by the coreduction of H_2PtCl_6 and $HAuCl_4$ with hydrazine. Particle size analysis indicated that the resultant bimetallic nanoparticles were monodispersed and had a mean diameter of 3−4.5 nm, depending on the composition of the feed solution. The smaller size of the bimetallic nanoparticles than the individual Au or Pt particles suggested that the nuclei for the bimetallic system might contain both Au and Pt, and the number of Au and Pt atoms required for the formation of nuclei might be less due to the different interaction of Au−Au, Pt−Pt, and Au−Pt. The comparison of the UV/vis absorption spectra for the bimetallic system and the physical mixture of individual metal nanoparticles revealed the formation of bimetallic nanoparticles. The XRD analysis also suggested the formation of bimetallic nanoparticles and revealed that the composition of each bimetallic particle was propor-

tional to that of the feed solution. The EDX analysis confirmed directly the formation of bimetallic nanoparticles and showed that the composition for each particle was roughly consistent with that of the feed solution. The XPS data indicated that the Pt atoms were enriched on the surface of the bimetallic nanoparticles, suggesting a structure of Au-core/Pt-shell. It was also shown that the surface composition of Au/Pt bimetallic nanoparticles had a linear relationship to the composition of the feed solution. The control of surface composition is of great interest and may be very important for the preparation of catalysts. In addition, the formation rate of the Au nanoparticles was found to be much faster than that of the Pt nanoparticles. According to the kinetic analysis and the characterization of the particles, the formation process of the Au/Pt bimetallic nanoparticles could be described. This study proposes another practical method for the preparation of Au/Pt bimetallic nanoparticles and should be helpful for the clarification of the formation process of Au/Pt bimetallic nanoparticles in w/o microemulsions.

Acknowledgment. This work was performed under the auspices of the National Science Council of the Republic of China, under Contract NSC 89-2214-E006-021, to which the authors express their thanks.

CM0006502